Catalysis Letters 64 (2000) 191–196

# Dynamic states of V-oxide species: reducibility and performance for methane oxidation on $V_2O_5/SiO_2$ catalysts as a function of coverage

M.A. Bañares[a,*], J.H. Cardoso[b], F. Agulló-Rueda[c], J.M. Correa-Bueno[b] and J.L.G. Fierro[a]

[a] *Instituto de Catálisis y Petroleoquímica, CSIC, Campus UAM-Cantoblanco, E-28049 Madrid, Spain*
E-mail: mbanares@icp.csic.es
[b] *Departamento de Engenharia Química, UFSCAR, São Carlos, São Paulo, Brazil*
[c] *Instituto de Ciencia de Materiales, CSIC, Campus UAM-Cantoblanco, E-28049 Madrid, Spain*

Received 16 July 1999; accepted 26 November 1999

Temperature-programmed *in situ* Raman spectroscopy is used to understand the effect of surface vanadia coverage on the structure, reducibility and performance for the oxidation of methane on $V_2O_5/SiO_2$ catalysts. The vanadia coverage on silica has no effect on its structure below its dispersion-limit loading ("monolayer" coverage); however, the interactions among surface vanadia species under reducing conditions become increasingly important. This interaction appears to operate through the sharing of oxygen sites facilitating the reduction, but it does not alter the total reducibility. The probability for this interaction to take place increases with vanadium oxide surface coverage. It is therefore expected that under reaction conditions the catalyst with higher vanadia coverage would have a greater capacity to release oxygen. This would increase the activity per vanadium site.

**Keywords:** supported vanadia, surface interaction, coverage effect, reducibility, methane oxidation, temperature-programmed Raman, TOF

## 1. Introduction

The direct conversion of methane to more valuable $C_1$ oxygenates is a very appealing route for the conversion of the large reserves of natural gas (>90% $CH_4$) [1,2]. Much work in this direction has been done in recent years, although the results reported so far have not always been encouraging [3,4]. It has been shown that the rate of destruction of HCHO on the catalyst surface is higher than in the gas phase [5]. We have recently reported that product distribution depends on the BET area of the support [6] and on the type of the redox oxide [7]. However, from a molecular point of view, the role of the coverage of a supported redox oxide in activity and selectivity is not fully understood. The TOF values for vanadia in a $V_2O_5/SiO_2$ series are affected by the coverage of vanadia on silica in the sub-"monolayer" region [8]. This is an unexpected result since the nature of the surface vanadium oxide species on silica is not affected by their surface coverage below its dispersion limit loading [9].

This work aims to explain the contradiction observed where the same sites afford different TOF numbers for methane conversion. *In situ* TP-Raman characterization provides valuable information about the behavior of surface vanadia sites at different coverage values under different conditions (catalytic reaction, TPR, TPO).

## 2. Experimental

Commercial non-porous silica (Aerosil 200, BET area 174 $m^2/g$, and particle size ca. 14 nm) was used as the starting material. Silica samples with lower BET areas were prepared by calcining several aliquots of the starting silica at temperatures in the 1273–1423 K range for a period between 3 and 9 h. The carriers were labeled "S$y$", where $y$ refers to the BET area of the support. S$y$ supports were impregnated with an aqueous solution of ammonium metavanadate (Aldrich) and hydrogen peroxide in a rotary evaporator at 343 K. The vanadium oxide concentration was close to 0.3 and 0.8 V atoms/$nm^2$ of the silica support, which is below monolayer capacity of vanadia on silica (ca. 1 V atom/$nm^2$). The impregnates were dried at 383 K and calcined in two steps: 623 K for 2 h and 923 K for 5 h. After calcination, they were sieved to a particle size from 0.125 to 0.250 mm diameter. The catalysts are referred to as "$x$V$y$"; in this case $x$ denotes the coverage of vanadium, expressed in vanadium atoms per $nm^2$ of the silica support.

The vanadium concentration of each sample was determined by atomic absorption spectrophotometry in a Perkin–Elmer 3030 instrument. The BET area of the catalysts was calculated by the BET method from the $N_2$ adsorption–desorption isotherms recorded at 77 K in a Micromeritics ASAP 2000 apparatus. XP spectra were obtained using an ESCALAB 200R spectrometer fitted with a hemispherical electron analyzer and a Mg anode X-ray exciting source

---

[*] To whom correspondence should be addressed.

(Mg K$\alpha$ = 1253.6 eV) powered at 120 W. All binding energies (BE) were referenced to the Si 2p peak at 103.4 eV.

Steady-state reaction experiments were carried out at atmospheric pressure in a 10 mm i.d. quartz fixed-bed microcatalytic reactor, designed to minimize the void volume upstream and downstream from the bed of the catalyst, which grants a linear increase of conversion with residence time at differential conditions. The advantages of this configuration have been described elsewhere [6,9]. The reactor feed was $CH_4$ (99.95 vol%) and $O_2$ (99.98 vol%) without diluent. The $CH_4/O_2$ molar ratio was adjusted to 2 by means of mass flow controllers (Brooks). The pseudo-residence time of methane was kept in the 0.3–2.0 g h/mol range, and reaction temperatures in the 783–983 K range. The experimental conditions and blank tests have been reported elsewhere [6].

TPR experiments were recorded with a Micromeritics equipment, model TPR/TPD-2900, fitted with a TCD and controlled by a computer. The samples (25 mg) were pretreated at 423 K in helium for 1 h. TPR experiments were run in a 10% $H_2$/Ar stream, heating the sample at a rate of 4 K/min. *In situ* temperature-programmed Raman (TP-Raman) experiments were run with a hot stage (Linkam TS-1500) that can be heated up to ca. 1800 K under flowing gases. The hot stage was attached to a Renishaw system-1000 microscope Raman spectrometer with an $Ar^+$ laser as exciting source at 514 nm. TP-Raman experiments were run by heating the sample from 323 to 973 K in steps of 50 K. Spectra were acquired over 5 min at each temperature, with a resolution of 2 $cm^{-1}$. 10% $H_2$ in Ar (SEO-L'Air Liquide) was used for the TPR-Raman experiments and synthetic air (SEO-L'Air Liquide) for the TPO-Raman experiments. The area of representative Raman bands has been integrated for all the spectra while only selected spectra are presented to illustrate the trends.

## 3. Results

Vanadia loading on the catalysts was decreased with the BET area of the support so that a nominal surface density of 0.3 and 0.8 V atoms/$nm^2$ on the silica support was maintained throughout the series. The V/Si XPS atomic ratio (table 1) indicated that the relative vanadia coverage was fairly constant within the 0.3V$y$ and 0.8V$y$ series. Raman spectra of dehydrated samples showed that on all the series, the supported vanadium oxide is present as isolated vanadia species, characterized by a Raman band near 1037 $cm^{-1}$.

Table 1
Chemical and surface analysis (XPS) of the silica-supported vanadia catalysts.

| Catalyst | $V_2O_5$ (wt%) | Nominal surface density (V atoms/$nm^2$) | V/Si XPS |
|---|---|---|---|
| 0.8V200 | 2.36 | 0.8 | 0.05 |
| 0.8V95 | 1.13 | 0.8 | 0.06 |
| 0.8V25 | 0.30 | 0.8 | 0.05 |
| 0.3V200 | 0.90 | 0.3 | 0.02 |
| 0.3V95 | 0.43 | 0.3 | 0.03 |
| 0.3V25 | 0.11 | 0.3 | 0.02 |

At a given conversion, the selectivity did not appear to follow a clear trend with vanadia coverage (table 2). The strongest effect on product distribution arises from the BET area of the catalysts since the formation of $C_2$ hydrocarbons is more evident for the catalysts with lower area. This has been studied in detail previously [6,11]. Figure 1 shows the TOF numbers of the $x$V200 and $x$V25 catalyst series. The TOF values increased with the surface vanadia coverage. However, it is interesting to note that vanadia on silica at sub-monolayer loading remains as surface isolated vanadia species. Raman, XANES and $^{51}$V-NMR *in situ* spectroscopy have shown that there are no polymeric vanadia species below monolayer coverage on silica under dehydrated conditions [9]. *In situ* spectroscopy under reaction conditions shows that the structure remains like that of the dehydrated system [10]. Therefore, vanadia coverage does not affect the structure of the vanadia site under dehydrated conditions and it does not have a clear effect on the selectivity but it does have a strong effect on the activity. The apparent contradiction that the active site re-

Table 2
Selectivity at 5% conversion on $V_2O_5/SiO_2$ catalyst series.[a]

| Catalyst | Temperature (K) | Selectivity (%) | | |
|---|---|---|---|---|
| | | $C_1$ oxygenates | $C_2H_n$ | $CO_x$ |
| 0.3V25 | 957 | 6.3 | 9.3 | 84.4 |
| 0.8V25 | 927 | 15.0 | 11.1 | 73.8 |
| 0.3V95 | 959 | 10.3 | 3.8 | 85.2 |
| 0.8V95 | 860 | 17.5 | 1.0 | 81.5 |
| 0.3V200 | 874 | 20.2 | 0.2 | 79.7 |
| 0.8V200 | 823 | 8.9 | 0.4 | 90.7 |

[a] Reaction conditions: 10 mm i.d. reactor, 200 mg, $W/F$ = 2 g h/mol, $CH_4/O_2$ = 2.

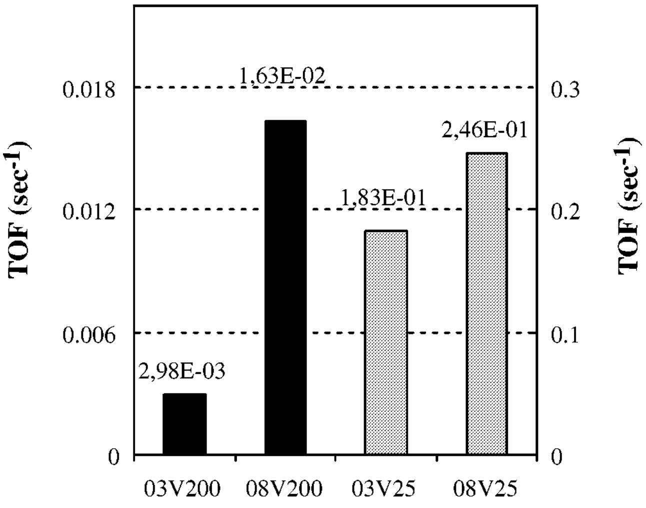

Figure 1. TOF values on $x$V200 and $x$V25 catalyst series at 823 and 943 K, respectively. Reaction conditions: 10 mm i.d. reactor, 200 mg, $W/F$ = 2 g h/mol, $CH_4/O_2$ = 2.

Table 3
Data of the TPR of the $V_2O_5/SiO_2$ catalyst series.

| Catalyst | V atoms/nm$^2$ | $T_{max}$ (K) | $E_a$ (kJ/mol) | O/V[a] |
|---|---|---|---|---|
| 0.3V200 | 0.3 | 760 | 117 | 1.2 |
| 0.3V95 | 0.3 | 786 | 125 | 1.2 |
| 0.3V25 | 0.3 | 794 | 100 | 1.2 |
| 0.8V200 | 0.8 | 682, 777 | 46, 121 | 1.3 |
| 0.8V95 | 0.8 | 777 | 125 | 1.2 |
| 0.8V25 | 0.8 | 766 | 125 | 1.2 |

[a] Oxygen atoms removed per V atom.

mains identical with coverage, while the activity per site increases, has not been addressed previously in literature. The activity results show the performance of a catalyst under dynamic conditions (catalytic cycles). To explain this, it must be emphasized that the characterization was made under static conditions (dehydrated) and that the relevance of vanadia coverage must be linked to some differences in the catalytic cycles. Under catalytic conditions the surface vanadium sites undergo a redox cycle, and the surface coverage has an effect on it, as shown below.

The TPR profiles of 0.3V200 and 0.8V200 point to a significant difference (table 3, figure 2(A)). The temperature of the peak maximum of hydrogen consumption is close to 760 K for 0.3 V atoms/nm$^2$ series, whereas it shifts to somewhat lower temperature for the 0.8 V atoms/nm$^2$ series (ca. 681 K), near 80 K below the value for 0.3V200. The reduction at low temperature appears to be related to vanadia on a different site. The apparent activation energy for the reduction of the site associated with the peak at higher temperatures was close to 125 kJ/mol, while it was 46 kJ/mol for the peak near 682 K. This new site does not appear to correspond to a deeper reduction of the V sites, since the amount of oxygen consumed per V site increased only slightly (table 3). When the 0.8V200 catalyst was reoxidized in a TPO cycle and a second TPR was run, the reduction profile was similar to that of the catalyst with a lower vanadia loading and a weak maximum near 670 K (figure 2(A)).

*In situ* TP-Raman spectra provide some structural information about the V sites under redox cycles. Figure 3 shows representative spectra of the 0.3V200 sample during a TPR and a TPO cycle. The broad bands near 495, 606, 802, and 907 cm$^{-1}$ correspond to the silica support and that at 1037 cm$^{-1}$ is due to dehydrated surface isolated V oxide species. Since the latter disappeared as the reduction of vanadia progresses; the changes in its area are plotted vs. reduction temperature in figure 2(B). It can be noted that vanadia species characterized by the V=O Raman band at 1037 cm$^{-1}$ was fully restored during TPO treatment (figure 3(B)). However, the 0.8V200 sample underwent some structural modifications (figure 4): at 473 K new Raman bands near 146, 284, 702, and 994 cm$^{-1}$ (crystalline $V_2O_5$) appeared [9]. As temperature increased during the TPR, the Raman bands of crystalline vanadia became more evident and then disappeared. Figure 2(C) plots the area of the Raman band at 1037 and 990 cm$^{-1}$ vs. reduction temperature during the TPR-Raman experiment on 0.8V200. The maximum intensity of the band of crystalline vanadia is comparable to that of the isolated vanadia species band close to 1037 cm$^{-1}$. Crystalline vanadia displays a very intense Raman signal, greater than isolated vanadia, thus suggesting that the size of the crystal is rather small, below the detection by XRD (<4 nm). Therefore, the relative intensity of the Raman bands of $V_2O_5$ crystallites as compared to that of isolated vanadium oxide species does not reflect the relative concentration of both kinds of surface vanadia species. The Raman band of isolated vanadium oxide species at 1037 cm$^{-1}$ persisted up to 823 K (figure 4(A)). The TPO-Raman spectra underlined the formation of both crystalline $V_2O_5$ and isolated vanadium oxide species. Therefore, the 0.8V200 sample does not undergo a reversible modification under redox cycles, whereas the 0.3V200 does.

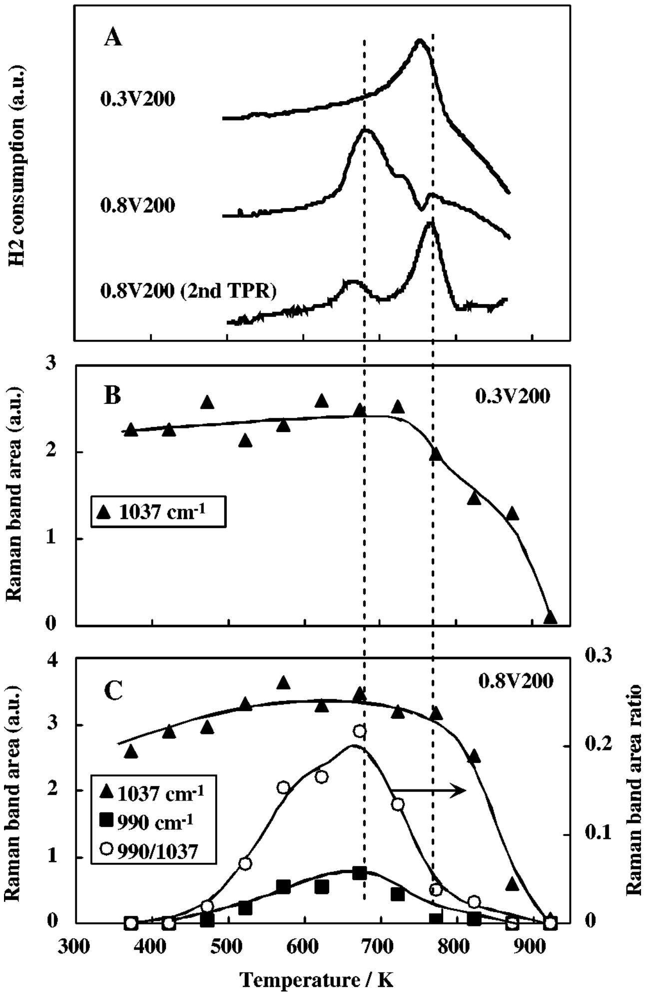

Figure 2. TPR profiles and TPR-Raman band areas of the 0.3V200 and 0.8V200 catalysts; and second TPR on 0.8V200 after a TPO experiment.

## 4. Discussion

The reduction maxima observed in the TPR profiles parallel the structural changes observed by *in situ* TP-Raman

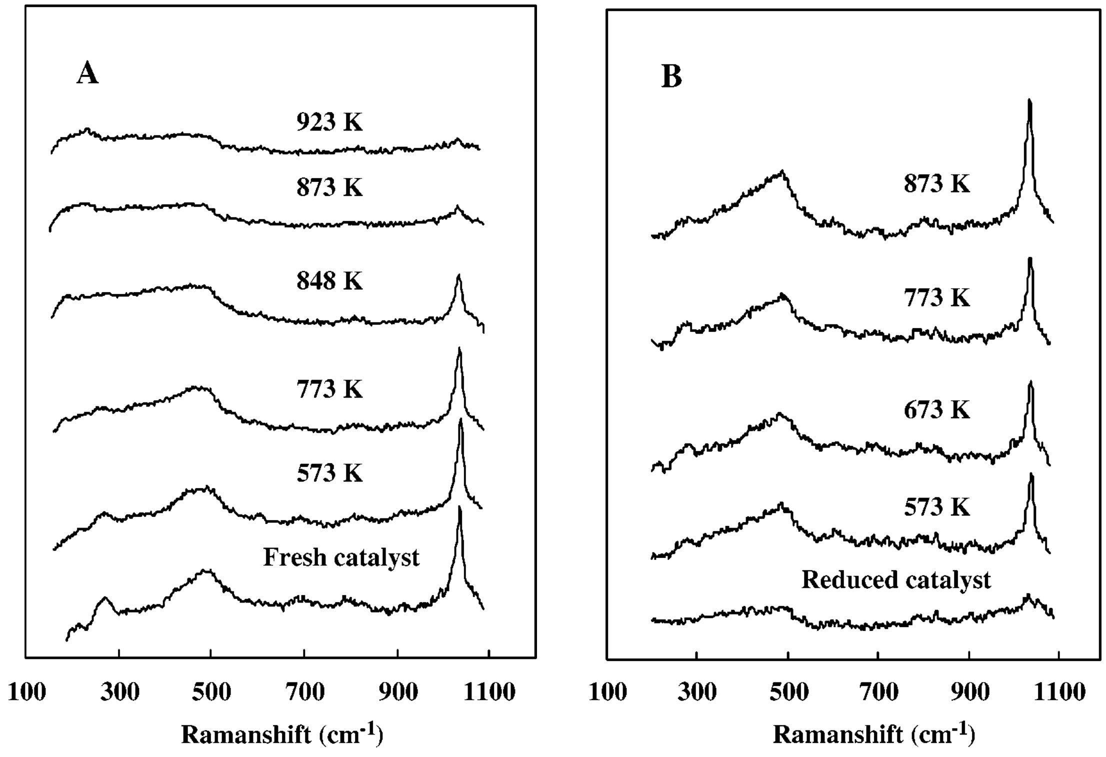

Figure 3. Selected Raman spectra of the 0.3V200 catalyst during the TPR Raman of a fresh sample (A) and during the TPO Raman of the reduced sample (B).

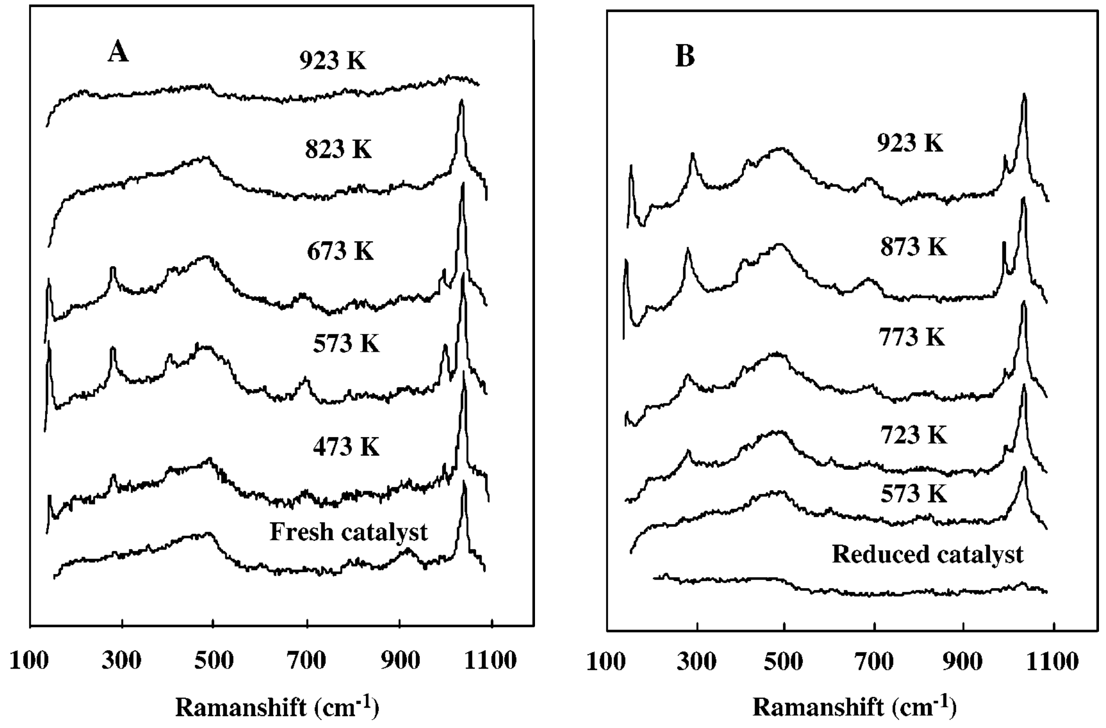

Figure 4. Selected Raman spectra of the 0.8V200 catalyst during the TPR Raman of a fresh sample (A) and during the TPO Raman of the reduced sample (B).

spectra: 0.3V200 shows a single reduction maximum which corresponds to the disappearance of surface isolated vanadium (V) oxide species, characterized by a Raman band near 1037 $cm^{-1}$ (figure 2(B)). The area of this Raman band for 0.3V200 remains constant up to ca. 750 K, and then sharply decreases. On the other hand, 0.8V200 presents a clearly different TPR profile. The first maximum near 680 K corresponds with the maximum formation of crys-

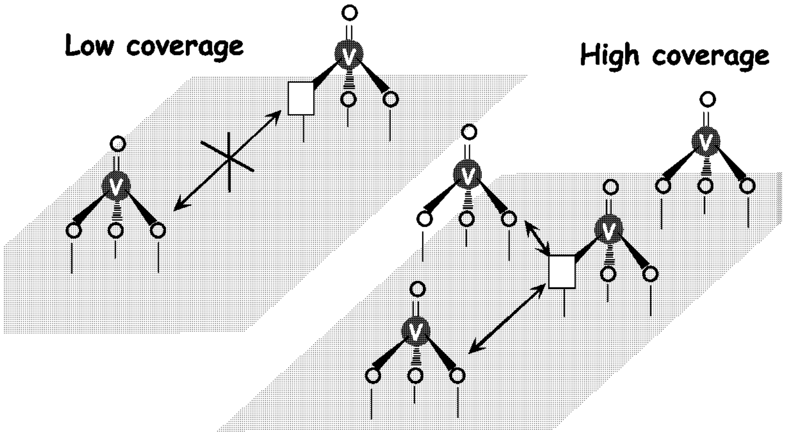

Scheme 1. Effect of vanadia coverage on the reducibility of $V_2O_5/SiO_2$ catalysts.

talline $V_2O_5$ (representative Raman band at 990 $cm^{-1}$ in figure 2(C)) from surface isolated vanadium oxide species. The shoulder near 727 K can be due to some reduction of the $V_2O_5$ crystallites, as observed by Koranne et al. [12] and parallels the decrease of the Raman band of crystalline vanadia (Raman band at 990 $cm^{-1}$ in figure 2(C)). The third TPR maximum near 770 K of 0.8V200 is close to that of 0.3V200 and corresponds to the reduction of surface isolated vanadium oxide species on silica, as the Raman spectra evidence (figure 4(A) and Raman band 1037 $cm^{-1}$ in figure 2(C)). The reoxidation of 0.8V200 after TPR regenerates both, crystalline and isolated vanadium oxide species (figure 4(B)). As underlined before, the amount of crystalline $V_2O_5$ is significantly lower than that of surface isolated vanadium oxide species. A TPR of the reoxidized 0.8V200 (figure 2(A)) shows two reduction maxima near 680 and 770 K, which correspond to the reduction of the $V_2O_5$ crystallites and to the reduction of surface isolated vanadium oxide species, respectively.

Vanadia coverage on silica of 0.3 or 0.8 V atoms/$nm^2$ has no effect on the structures of the site, as measured by Raman spectroscopy, but it does have a strong effect on catalytic performance and reducibility. The reduction is more difficult at low vanadia coverage than at high surface vanadia coverage, as highlighted by the TPR profiles. *In situ* Raman spectroscopy reveals a rearrangement of surface vanadia species under reduction at loading values close to its dispersion limit. The surface structure of the fresh catalyst is fully restored after a TPR/TPO cycle for the low vanadia coverage. Vanadium oxide species have some mobility, but they do not tend to aggregate since dispersion provides a lower surface free energy relative to the high free energy of the exposed oxide supports [13,14]. However, under reducing conditions, the removal of oxygen should be considerably easier for vanadia species able to compensate O-removal by sharing oxygen sites. The chances for this interaction among surface vanadia sites should increase with the vanadia coverage (scheme 1). Furthermore, this process means no reduction for the vanadium sites despite hydrogen is consumed. The ability of vanadia sites to interact among them is very low at low coverage because of the high average distance among them; however, as coverage increases, the average distance among vanadia sites decreases, thus favoring interactions. V–O–V bonds would be developed in order to compensate the loss of an oxygen atom, thus leading to the formation of surface polymeric vanadia species. However, Das et al. [9] have shown by Raman, XANES and $^{51}$V-NMR that vanadia on silica may exist in two extreme configurations: surface isolated vanadia species and crystalline $V_2O_5$, but not as polymeric species. Since silica is unable to stabilize dehydrated polymeric vanadia structures, any effect that promotes interactions among surface vanadia species must lead to the formation of crystalline $V_2O_5$, as reflected by the TPR-Raman experiments on 0.8V200. After a TPR/TPO cycle the second TPR profile has a small low-temperature reduction maximum and a large high-temperature reduction maximum (figure 2(A)), in agreement with the presence of small crystals of $V_2O_5$ along with larger amounts of isolated vanadium oxide species (figure 4(B)). This must be due to the decrease in vanadia coverage due to the aggregation of part of the vanadia surface species into $V_2O_5$ crystallites. The presence of a small amount of crystalline $V_2O_5$ accounts for the reduction maximum near 664 K, while the more intense reduction maximum near 770 K is due to surface isolated vanadium oxide species. The different characteristics induced on the surface vanadia species on silica upon increasing coverage enables the formation of vanadia crystallites, which must endow the oxygen sites with different reactivities. Thus, the higher capacity to release oxygen under less reducing conditions may lead to a higher activity per site that would account for the increase of TOF number values with vanadia coverage on silica.

## 5. Conclusions

The TPR profiles and *in situ* TP-Raman spectra reveal the interaction among surface vanadia species under reducing conditions through the sharing of oxygen sites. The chances for this interaction to occur must be directly related to the surface vanadia density. This effect does not alter the total reducibility, as shown by the O/V ratios in TPR experiments, but does facilitate the reduction, as suggested by the shift of temperatures in the TPR profiles and the different apparent activation energy values. It is therefore expected that under catalytic oxidation reaction conditions the 0.8V200 catalyst would have a greater capacity to release oxygen, which would account for its higher activity.

## Acknowledgement

The authors appreciate valuable discussions with Dr. M. Faraldos. This research was partially supported by the Commission of the European Union under grant JOU2-CT92-0040 and the Comisión Interministerial de Ciencia y Tecnología (CICYT), Spain, under projects 95-0894. CICYT Grant IN96-0053 funded the acquisition of the Raman spectrometer. JHC thanks FAPESP and CAPES (Brazil) for a scholarship grant for his stay in Spain.

## References

[1] N.R. Foster, Appl. Catal. 19 (1985) 1.
[2] M.J. Brown and N.D. Parkyns, Catal. Today 8 (1981) 305.
[3] T.R. Baldwin, R. Burch, G.D. Squire and S.C. Tsang, Appl. Catal. 74 (1991) 137.
[4] C.S. Walker, J.A. Lapszewicz and G.A. Foulds, Catal. Today 21 (1994) 519.
[5] S. Irusta, E.A. Lombardo and E.E. Miró, Catal. Lett. 24 (1994) 339.
[6] F. Martín-Jiménez, J.M. Blasco, L.J. Alemany, M.A. Bañares, M. Faraldos, M.A. Peña and J.L.G. Fierro, Catal. Lett. 33 (1995) 279.
[7] M.A. Bañares, L.J. Alemany, M. López Granados, M. Faraldos and J.L.G. Fierro, Catal. Today 33 (1997) 73.
[8] M.S. Faraldos, M.A. Bañares, J.A. Anderson, I.E. Wachs and J.L.G. Fierro, J. Catal. 160 (1996) 214.
[9] N. Das, H. Eckerdt, H. Hu, I.E. Wachs, J.F. Walzer and F.J. Faher, J. Phys. Chem. 97 (1993) 8240.
[10] Q. Sun, J.-M. Jehng, H. Hu, R.G. Herman, I.E. Wachs and K. Klier, J. Catal. 165 (1997) 91.
[11] J.H. Cardoso, M.A. Bañares, J.M. Correa-Bueno and J.L.G. Fierro, Collect. Czech. Chem. Commun. 63 (1998) 1743.
[12] M.M. Koranne, J.G. Goodwin and G. Marcelin, J. Catal. 148 (1994) 369.
[13] H. Knözinger and E. Taglauer, Catalysis 10 (1993) 1.
[14] C.B. Wang, Y. Cai and I.E. Wachs, Langmuir 15 (1999) 1223.